Structural Engineering and Mechanics, Vol. 14, No. 1 (2002) 85-98
DOI: http://dx.doi.org/10.12989/sem.2002.14.1.085

Parametric study for buildings with combined displacement-dependent and velocity-dependent energy dissipation devices

W.S. Pong†

Department of Civil Engineering, School of Engineering, San Francisco State University, 1600 Holloway Avenue, San Francisco, California 94132, U.S.A.

C.S. Tsai‡, Ching-Shyang Chen‡† and Kuei-Chi Chen‡†

Department of Civil Engineering, Feng Chia University, Taichung, Taiwan

(*Received October 23, 2001, Accepted April 11, 2002*)

Abstract. The use of supplemental damping to dissipate seismic energy is one of the most economical and effective ways to mitigate the effects of earthquakes on structures. Both displacement-dependent and velocity-dependent devices dissipate earthquake-induced energy effectively. Combining displacement-dependent and velocity-dependent devices for seismic mitigation of structures minimizes the shortcomings of individual dampers, and is the most economical solution for seismic mitigation. However, there are few publications related to the optimum distributions of combined devices in a multiple-bay frame building. In this paper, the effectiveness of a building consisting of multiple bays equipped with combined displacement-dependent and velocity-dependent devices is investigated. A four-story building with six bays was selected as an example to examine the efficiency of the proposed combination methods. The parametric study shows that appropriate arrangements of different kinds of devices make the devices more efficient and economical.

Key words: velocity-dependent devices; displacement-dependent devices; energy dissipation devices; supplemental damping.

1. Introduction

The loss of life and property, destruction of major infrastructure, and severe economic disruption from earthquakes, is enormous in many earthquake-prone areas. Repair costs for infrastructure damage alone from the 1989 Loma Prieta and 1994 Northridge earthquakes were substantial. Since the Northridge earthquake in 1994 and the Kobe earthquake in 1995, many discoveries have been made in the area of earthquake engineering. As a result, seismic structural design methods and engineering practices are undergoing constant innovations. Rapid changes in seismic design

† Assistant Professor
‡ Professor
‡† Research Assistant

concepts and practices are due to discoveries about earthquake ground motion behavior and the development of many innovative control theories. Many advanced technologies have also become available in recent years. Considerable progress has been made over the last two decades in structural control (Soong 1998).

The concept behind passive control is to add energy-dissipating devices to a structure. The use of energy devices to dissipate seismically induced energy is one of the most economical and effective ways to mitigate the effects of earthquakes on buildings. In recent years, great effort has been made to develop energy-dissipation devices by various investigators.

Based on their mechanical behavior, energy-absorbing devices may be classified into velocity-dependent and displacement-dependent devices (FEMA-273, 1997). Velocity-dependent devices are so characterized because the forces developed during their operation are dependent upon velocity. Included in this class of energy dissipation devices are viscoelastic solid, viscoelastic fluid (Mahmoodi 1972, Aiken *et al.* 1990, Zhang and Soong 1992, Tsai 1993 & 1994, Tsai and Lee 1993 & 1994, Pong and Tsai 1995), and viscous fluid dampers (Constantionou and Symans 1992, Pong 1998). For these devices, the response changes at different excitation frequencies, indicating their rate dependence (FEMA-273, 1997). Another characteristic of these devices is that energy dissipation occurs even for extremely small deformations, making them suitable for controlling wind as well as seismic disturbances.

On the other hand, the response of displacement-dependent devices is substantially independent of the relative velocity between each end of the devices, and of the frequency of the excitation (FEMA-273, 1997). Their response is primarily a function of the relative displacement between each end of the device. This classification of passive devices includes friction dampers (Aiken *et al.* 1988, Pall *et al.* 1991, Pekau and Guimond 1991) and metallic yielding devices (Skinner *et al.* 1975, Kelly and Skinner 1980, Stiemer and Chow 1984, Whittaker *et al.* 1989, Bergman and Hanson 1990, Tsai and Chung 1998).

Viscoelastic dampers and fluid viscous dampers may fail to reduce structural responses at the early stage (first few seconds) of earthquakes (Tsai and Lee 1993 & 1994). However, friction dampers and metallic energy absorbers, may not provide sufficient supplemental damping to the structure during minor earthquake loadings (Pong *et al.* 1994).

As is shown in Fig. 1, viscoelastic (VE) dampers (Keel and Mahmoodi 1986) have been adopted for several tall buildings in the U.S. to reduce wind-induced responses. In recent years, analytical

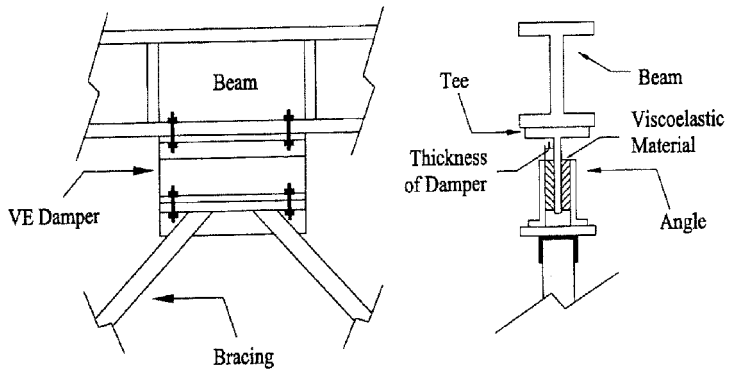

Fig. 1 Detail of VE damper

and experimental research has demonstrated their effectiveness for seismic hazard mitigation of buildings. The major advantage of using VE dampers as energy-absorbing devices for seismic hazard mitigation is that energy can be dissipated under arbitrary earthquake loadings. However, structural responses cannot be reduced significantly at the early stage of ground motions by VE dampers (Tsai and Lee 1993 & 1994, Pong 1994). The reason for this phenomenon is that the behavior of a VE damper possesses velocity dependence that is regarded as unfavorable in such devices, because of zero or small velocities at and in the vicinity of peak displacements.

The reinforced added damping and stiffness device (RADAS) (Tsai and Chung 1998) has been tested as a very reliable energy absorbing device for seismic hazard mitigation, as shown in Fig. 2. RADAS is classified as a displacement-dependent device. There are several advantages of using RADAS devices to resist earthquake damage: (1) energy dissipation can be constrained to the location of the RADAS devices; (2) a substantial reduction in the energy dissipation demands on the structure; (3) the devices can be replaced easily after a severe seismic event; and (4) the devices can provide the building with stiffness and strength as well as increased energy dissipation capacity.

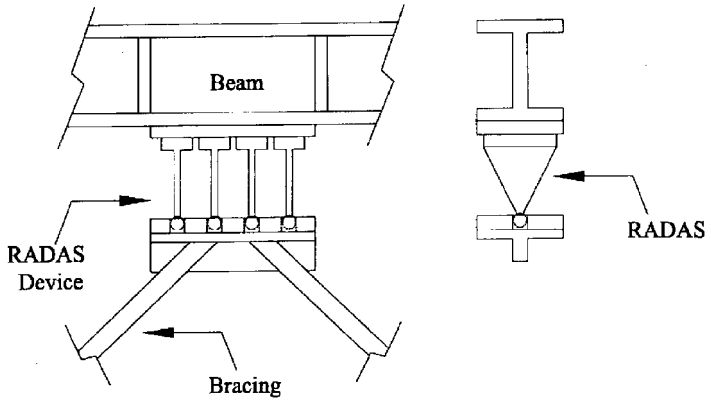

Fig. 2 Detail of RADAS device

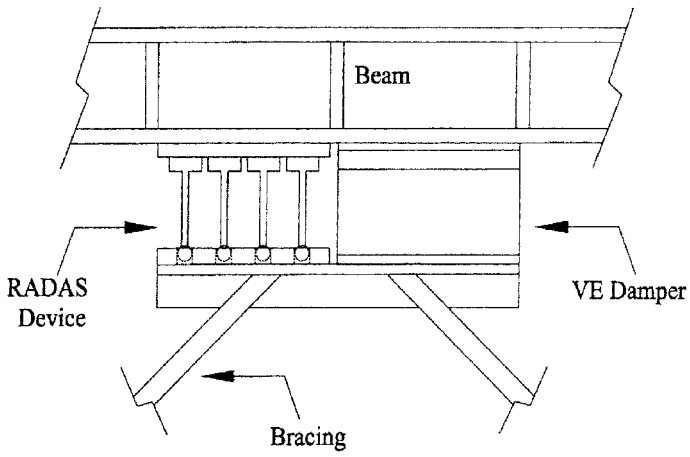

Fig. 3 Detail of combined device

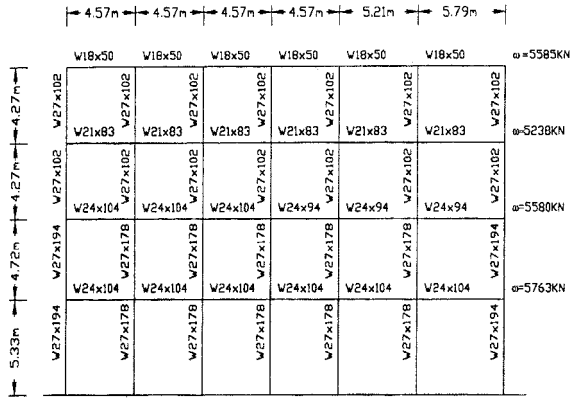

Fig. 4 A 4-story of steel frame with multiple bays

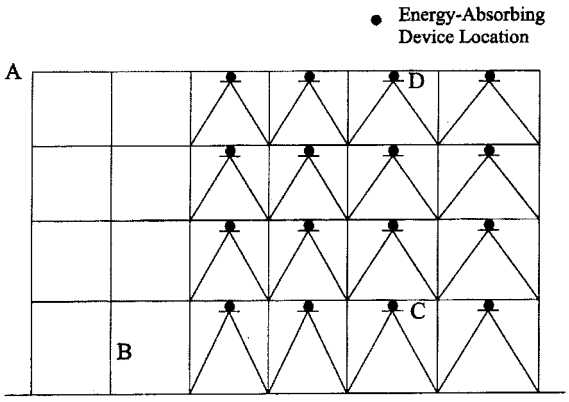

Fig. 5 Designated locations of energy-absorbing devices

However, RADAS devices behave more as stiffeners than as dampers during minor earthquakes.

The use of combined velocity-dependent and displacement-dependent devices (Pong *et al*. 1994, Tsai and Chen 1998) has been recognized as an effective way to increase the advantages and eliminate the disadvantages of the individual devices. However, there are no publications, to the best of the authors' knowledge, related to the optimum distributions of combined devices in a multiple bay building. This paper investigates the effectiveness of a building consisting of multiple bays equipped with combined devices, including VE dampers and RADAS devices, as shown in Fig. 3. A four-story building with six bays, as shown in Fig. 4, has been selected as an example to examine the efficiency of the proposed combined devices. The VE damper and RADAS are chosen as a sample of velocity-dependent and displacement-dependent devices, respectively, and they are mounted at the designated locations and supported by chevron braces, as shown in Fig. 5. This study shows that appropriate arrangements of different kinds of devices make the devices more effective and economic.

2. Analytical model for velocity-dependent damper

An analytical model developed by Tsai and Lee (1994) is adopted for the VE damper to account for the effects of temperature and earthquake loadings. The concept of fractional derivatives in the formulation of a stress-strain relationship for a viscoelastic material is employed.

The 3-parameter function derivative model was chosen for the constitutive model. The fractional calculus model of VE behavior is given by

$$\tau(t) = G_0\gamma(t) + G_1 D^{\alpha}[\gamma(t)] \tag{1}$$

$$D^{\alpha}[\gamma(t)] = \frac{1}{\Gamma(1-\alpha)}\frac{d}{dt}\int_0^t \frac{\gamma(\tau)}{(t-\tau)^{\alpha}}dt \quad 0<\alpha<1 \tag{2}$$

$$G_0 = G_1 = A_0\{1 + \mu e^{-\beta[\tau d\gamma + \theta(T-T_0)]}\} \tag{3}$$

in which $\tau(t)$ is shear stress; $\gamma(t)$ is shear strain; G_0 and G_1 are constitutive model parameters; $\acute{a}$, A_0,

â, í and *é* are unknown coefficients to be determined from the experimental data; T is the ambient temperature; and T_0 is the reference temperature at which the unknown coefficients are obtained.

If the linear variation of the shear strain between two time-steps, $(n-1)\Delta t$ and $n\Delta t$, is assumed, then the strain is expressed as

$$\gamma(\tau) = \left(n - \frac{\tau}{\Delta t}\right)\gamma[(n-1)\Delta t] + \left(\frac{\tau}{\Delta t} - (n-1)\right)\gamma(n\Delta t)$$
$$(n-1)\Delta t \le \tau \le n\Delta t \tag{4}$$

Substitution of Eq. (4) into Eq. (1) and Eq. (2) leads to the constitutive law for the viscoelastic damper at time step $N\Delta t$; that is

$$\tau(N\Delta t) = \left[G_0 + \frac{G_1(\Delta t)^{-\alpha}}{(1-\alpha)\Gamma(1-\alpha)}\right]\gamma(N\Delta t) + F(N\Delta t)$$
$$= \left[G_0 + \frac{G_1(\Delta t)^{-\alpha}}{\Gamma(2-\alpha)}\right]\gamma(N\Delta t) + F(N\Delta t) \tag{5}$$

In the above equation, the previous time effect of the strain $F(N\Delta t)$, is defined as

$$F(N\Delta t) = \frac{G_1(\Delta t)^{-\alpha}}{\Gamma(2-\alpha)}\{[(N-1)^{1-\alpha} + (-N+1-\alpha)N^{-\alpha}]\gamma(0)$$
$$+ \sum_{n=1}^{N-1}[-2(N-n)^{1-\alpha} + (N-n+1)^{1-\alpha} + (N-n-1)^{1-\alpha}]\gamma(n\Delta t)\} \tag{6}$$

3. Analytical model for RADAS device

A two-surface model (Tsai and Tsai 1995), as shown in Fig. 6, is adopted so that the behavior of the RADAS device subjected to earthquake loadings can be predicted accurately. The analytical model has been verified by experimental results (Tsai and Chung 1998) and will be described

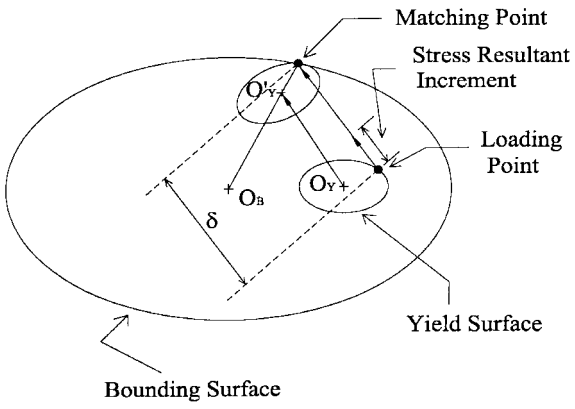

Fig. 6 Two-surface model for nonlinear plasticity

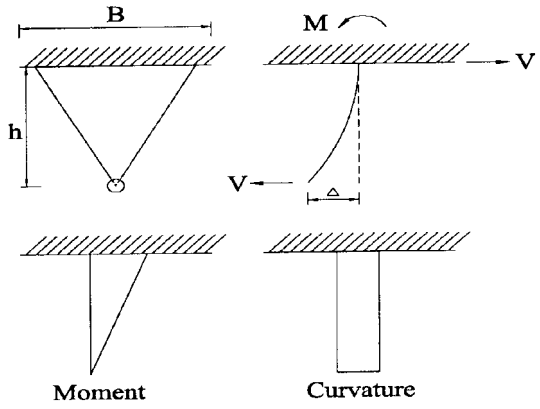

Fig. 7 Basic behavior of RADAS device

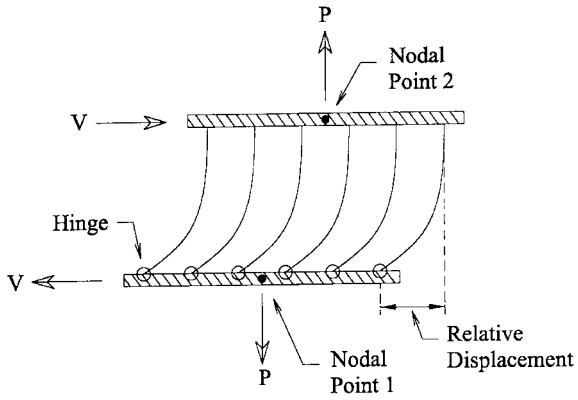

Fig. 8 Mechanical behavior of RADAS device

briefly in the following section.

When a finite displacement is imposed in the end of the triangular plate, as shown in Fig. 7, the curvature is a uniform distribution over the height. Therefore, the yielding can occur simultaneously in the entire plate without curvature concentrations, and the bending moment at the free end of the plate is equal to zero.

The generalized stress resultant $\boldsymbol{F}$, for the general case of a RADAS element as shown in Fig. 8, may be written as:

$$\boldsymbol{F}^T = [P,\ V] \tag{7}$$

in which P is the axial force (if the axial force exists); and V is the transverse shear force. It should be noted that the flexural characteristics of the RADAS element are a function of the transverse shear force V, and the axial force P may be zero.

The modified elastic stiffness $\boldsymbol{K}_{ep}$ due to the plastic flow and can be expressed as

$$\boldsymbol{K}_{ep} = \boldsymbol{K}_e - \frac{\boldsymbol{K}_e \boldsymbol{n}\boldsymbol{n}^T \boldsymbol{K}_e}{\boldsymbol{n}^T \boldsymbol{K}_e \boldsymbol{n} + \boldsymbol{n}^T \boldsymbol{K}_p \boldsymbol{n}} \tag{8}$$

in which $\boldsymbol{K}_e$ is a 2×2 diagonal matrix of elastic modulus from the individual force-deformation relationship. If K_e^a and K_e^v are elastic moduli for the axial and transverse directions, respectively, then $\boldsymbol{K}_e$ is given by

$$\boldsymbol{K}_e = diag\left|K_e^a,\ K_e^v\right| \tag{9}$$

In Eq. (8), $\boldsymbol{K}_p$ is a 2×2 diagonal matrix of generalized plastic modulus from the individual force-deformation relationship. If K_p^a and K_p^v represent this relationship in the axial and transverse directions, respectively, then $\boldsymbol{K}_p$ can be expressed as

$$\boldsymbol{K}_p = diag\left|K_p^a,\ K_p^v\right| \tag{10}$$

Assume that the yield function ϕ for the RADAS element is given by

$$\phi = a\left(\frac{P}{P_u} - \frac{X_1}{P_u}\right)^2 + \left(\frac{V}{V_u} - \frac{X_2}{V_u}\right)^2 - \kappa_\beta^2 = 0 \tag{11}$$

then $\phi_{,F}$ may be expressed as

$$\phi_{,F} = \begin{Bmatrix} \frac{2a}{P_u}\left(\frac{P}{P_u} - \frac{X_1}{P_u}\right) \\ \frac{2}{V_u}\left(\frac{V}{V_u} - \frac{X_2}{V_u}\right) \end{Bmatrix} \tag{12}$$

in which P_u = the axial force to cause the RADAS element fully plastified; V_u = the transverse shear force to cause the RADAS element fully plastified; X_1 = current offset of the yield surface in the axial force direction; X_2 = current offset of the yield surface in the transverse shear force direction; and κ_β = size of the yield surface.

The unit outward normal vector $\boldsymbol{n}$ to the yield surface is given by

$$\boldsymbol{n} = \frac{\phi_{,F}}{[\phi_{,F}^T \cdot \phi_{,F}]^{1/2}} \tag{13}$$

$$\phi_{,F}^T = \left[\frac{\partial \phi}{\partial P}, \frac{\partial \phi}{\partial V}\right] \tag{14}$$

If one defines $N = [\phi_{,F}^T \cdot \phi_{,F}]^{1/2}$, then the unit normal direction, $\boldsymbol{n}$, is given as

$$\boldsymbol{n} = \begin{Bmatrix} n_1 \\ n_2 \end{Bmatrix} = \frac{1}{N}\begin{Bmatrix} \frac{2a}{P_u}\left(\frac{P}{P_u} - \frac{X_1}{P_u}\right) \\ \frac{2}{V_u}\left(\frac{V}{V_u} - \frac{X_2}{V_u}\right) \end{Bmatrix} \tag{15}$$

Let $S = \boldsymbol{n}^T \boldsymbol{K}_e \boldsymbol{n} + \boldsymbol{n}^T \boldsymbol{K}_p \boldsymbol{n}$, then

$$S = n_1^2[K_e^a + K_p^a] + n_2^2[K_e^v + K_p^v] \tag{16}$$

With the aid of Eq. (12)-(16), the $\boldsymbol{K}_{ep}$ of Eq. (8) can be obtained

$$\boldsymbol{K}_{ep} = \begin{bmatrix} K_e^a - \frac{(n_1 K_e^a)^2}{S} & \frac{-n_1 n_2 (K_e^a)(K_e^v)}{S} \\ \frac{-n_1 n_2 (K_e^a)(K_e^v)}{S} & K_e^v - \frac{(n_2 K_e^v)^2}{S} \end{bmatrix} \tag{17}$$

4. Theoretical elastic stiffness of RADAS elements

Assuming the base of the plate is fully restrained and neglecting the shear deformation, the theoretical elastic lateral stiffness of RADAS elements, K_e^v, can be expressed as

$$K_e^v = \frac{NEbt^3}{6h^3} \tag{18}$$

in which E is Young's modulus, N is the number of RADAS plates, t is the thickness of the plates, b is the base width of the plate, and h is the height of the plate.

According to the experimental results by Tsai and Chung (1998), the lateral elastic stiffness of RADAS elements in Eq. (18) was acceptable when selecting the properties of RADAS elements.

5. The seismic characteristic of the 4-story building frame

A 4-story 11,150 m^2 office building was designed in accordance with Uniform Building Code (UBC) 97 provision requirements based upon static analysis using the criteria that follow:

Seismic Zone Factor, Z	0.4
Important Factor, I	1.0
Site Coefficient	S_d
Seismic Source	A
Distance from Fault	12 km

The structural period, T_a, was estimated using the following formula, included as Method A in UBC 97 Section 1630.2.2:

$$T_a = C_t(h_n)^{3/4} \tag{19}$$

C_t is a coefficient equal to 0.035 for special moment resisting frame (SMRF), and h_n is the total building height. The value, T_a, obtained by Method A was 0.764 second. The value, T_b, was found by multiplying T_a by 1.3 (the maximum permissible per UBC 97, Method B). The calculated value of T_b was 0.993 second. This value of T_b was rounded up to one second for simplicity and used in subsequent calculations. In accordance with UBC 97 Section 1630.2, design base shear for the building was calculated using the following formula:

$$V = \frac{C_v IW}{RT} \tag{20}$$

where C_v is the seismic coefficient, I is the importance factor, W is the building weight, R is a factor based on ductility of structure type (in this case $R = 8.5$), and T is the building period. Fig. 4 shows the typical steel beam and column member sizes designed based on this information. Poisson's ratio and elastic modulus equal to 0.3 and 0.200×10^{12} N/m^2, respectively, were used for this study.

In the analysis, it is assumed that the floors were rigid in their own plane. The north-south ground motion component of the 1940 El Centro earthquake was selected for this study. Energy-absorbing devices are added on the designated locations as shown in Fig. 5. This study aims to propose the optimum design of structure equipped with energy-absorbing devices. When the structure is only equipped with VE dampers, the sizes of VE dampers on designated locations are shown in Table 1. When the structure is equipped only with RADAS devices, the sizes for RADAS devices on designated locations are shown in Table 2. When the structure is furnished with combined devices

Table 1 The properties of VE damper

	Thickness (cm)	Area (cm^2)
4F	0.76	3252
3F	0.76	3252
2F	0.76	3252
1F	0.76	3252

Table 2 Properties of RADAS

	B (cm)	*h* (cm)	Thickness (cm)	No. of Plates
4F	12.70	10.16	3.26	22
3F	12.70	10.16	3.26	22
2F	12.70	10.16	3.26	22
1F	12.70	10.16	3.26	22

Table 3 Properties of combined devices

	VE damper component		RADAS device component			
	Thickness (cm)	Area (cm^2)	*B* (cm)	*h* (cm)	Thickness (cm)	No. of Plates
4F	0.76	3252	12.70	10.16	3.26	22
3F	0.76	3252	12.70	10.16	3.26	22
2F	0.76	3252	12.70	10.16	3.26	22
1F	0.76	3252	12.70	10.16	3.26	22

(as shown in Fig. 3), the size of combined devices on every designated location is shown in Table 3. The structural response parameters include the floor displacement at point A, the column shear force at point B, the hysteresis loops of energy-absorbing device at point C and D. These parameters are also shown in Fig. 5.

6. Parametric study of structural seismic responses

The parametric studies demonstrate that the addition of different kinds of energy dissipation devices to a structure will yield various reduction effects on roof displacements during an earthquake. When VE dampers are selected to equip the designated locations, the roof displacements of the building could be reduced effectively, as is shown in Fig. 9. However, it could not lessen structural responses at the early stage of excitations due to its dependence on velocities. A few seconds later, responses have been improved. The displacement dependent devices such as RADAS can decrease the roof displacements of a structure at the beginning of a ground shaking, as is shown in Fig. 10. It was found that RADAS devices have good performance in strong earthquakes. If VE dampers as well as RADAS devices are constructed at the designated locations, the roof responses would be mitigated effectively, as is shown in Fig. 11. The combination method

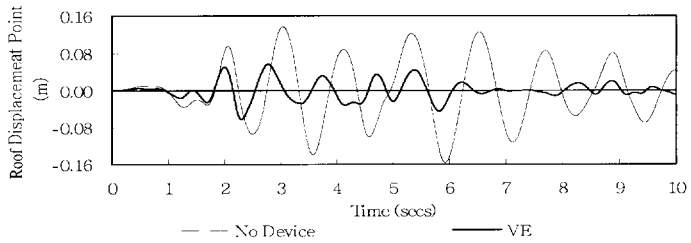

Fig. 9 Response of roof displacement when structure is equipped with VE damper during El Centro ground motion

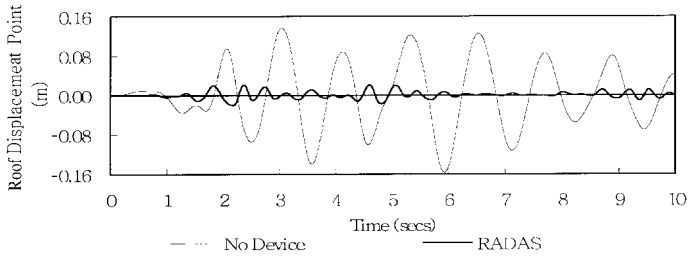

Fig. 10 Response of roof displacement when structure is equipped with RADAS device during El Centro ground motion

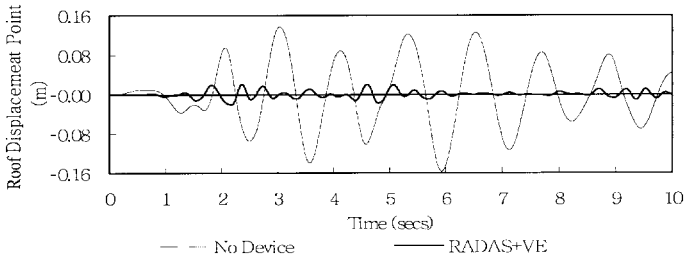

Fig. 11 Response of roof displacement when structure is equipped with combined device during El Centro ground motion

can also be applied to wind control.

In comparison with the shear forces at point B of the column, the reduction effects on the shear forces are also distinct for different energy-absorbing devices. As shown in Fig. 12, when VE dampers were constructed on the designated locations, the shear forces were reduced greatly. Nonetheless, it could not effectively lower structural responses at the early stage of excitations. The shear forces are diminished when RADAS devices are arranged on the designated locations as depicted in Fig. 13. This is because most earthquake induced energy is collected in the RADAS devices, and dissipated in great quantity by yielding the RADAS devices. If both VE dampers and RADAS devices are built together on the assigned locations, the shear forces at point B would be reduced more effectively, as is shown in Fig. 14.

In order to know whether the energy-absorbing devices performed properly, the hysteresis loops

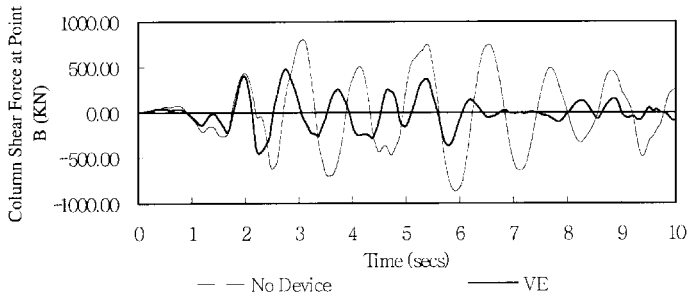

Fig. 12 Response of column shear force when structure is equipped with VE damper during El Centro ground motion

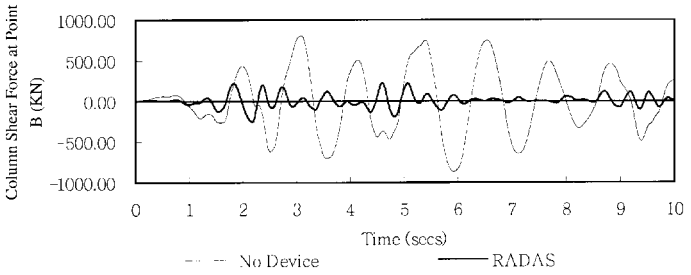

Fig. 13 Response of column shear force when structure is equipped with RADAS device during El Centro ground motion

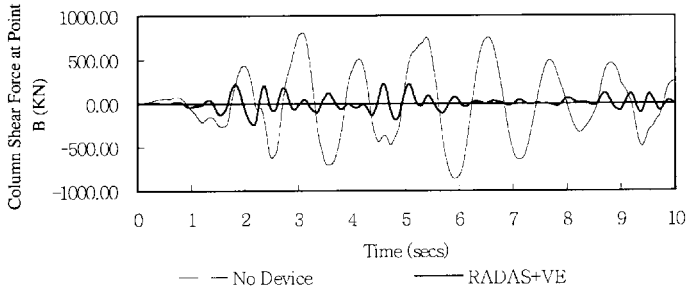

Fig. 14 Response of column shear force when structure is equipped with combined device during El Centro ground motion

of energy-absorbing devices at points C and D were investigated. When VE dampers are added on the designated locations, the hysteresis loops of VE dampers at points C and D are portrayed in Figs. 15 and 16, respectively. The VE dampers function effectively both on lower and upper stories, but they can dissipate more energy on lower stories. This is because earthquake induced energy is larger on lower stories than on upper stories. When RADAS devices are added on the designated locations, the hysteresis loops of RADAS devices at points C and D are displayed in Figs. 17 and 18, respectively, showing that RADAS devices can dissipate energy effectively on lower stories. However, they do not yield on upper stories. Therefore, they would behave as stiffeners rather than energy dissipaters. If both of the RADAS devices and VE dampers are at the designated locations,

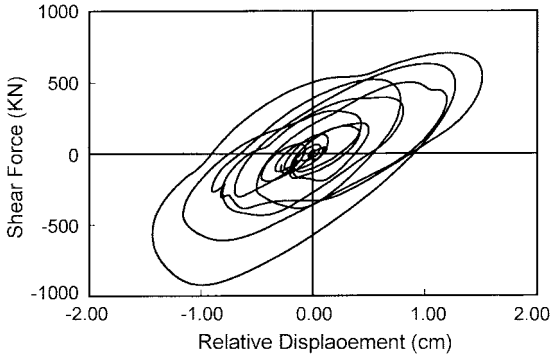

Fig. 15 Hysteresis loop of VE damper at point C when structure is equipped with VE damper during El Centro ground motion

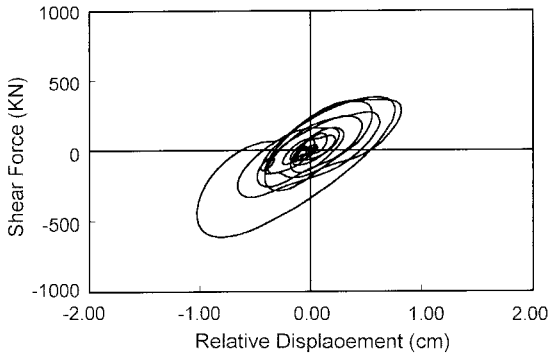

Fig. 16 Hysteresis loop of VE damper at point D when structure is equipped with VE damper during El Centro ground motion

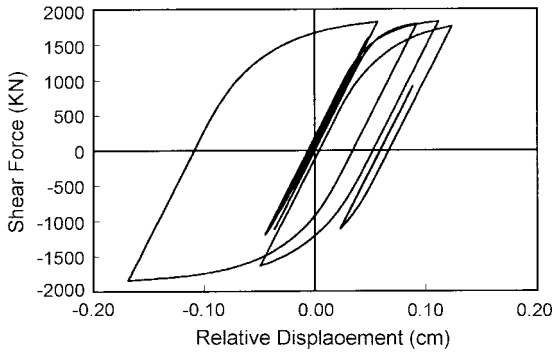

Fig. 17 Hysteresis loop of RADAS device at point C when structure is equipped with RADAS device during El Centro ground motion

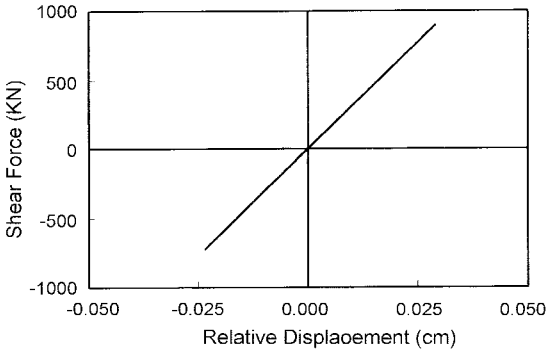

Fig. 18 Hysteresis loop of RADAS device at point D when structure is equipped with RADAS device during El Centro ground motion

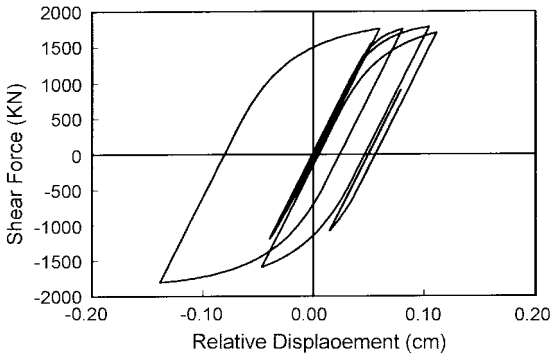

Fig. 19 Hysteresis loop of RADAS device at point C when structure is equipped with combined device during El Centro ground motion

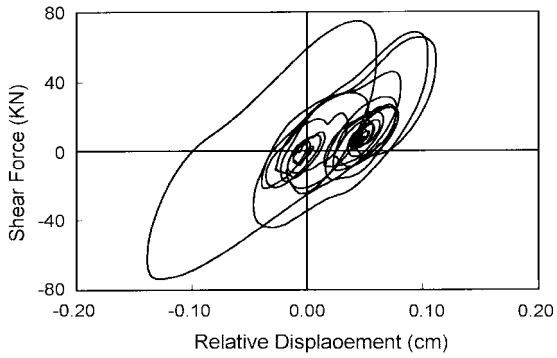

Fig. 20 Hysteresis loop of VE damper at point C when structure is equipped with combined device during El Centro ground motion

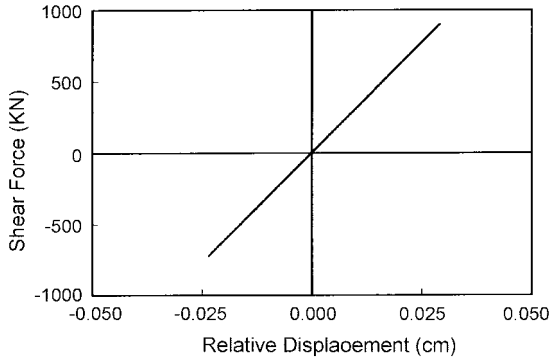

Fig. 21 Hysteresis loop of RADAS device at point D when structure is equipped with combined device during El Centro ground motion

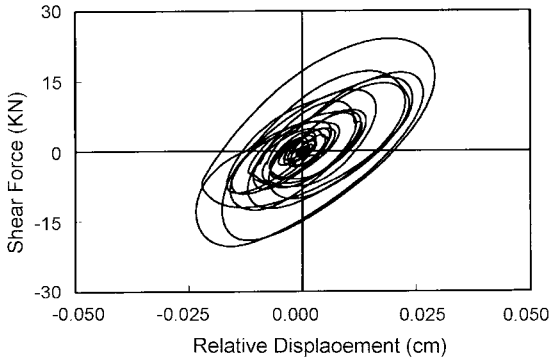

Fig. 22 Hysteresis loop of VE damper at point D when structure is equipped with combined device during El Centro ground motion

the hysteresis loops of VE dampers and RADAS devices at points C and D appear in Figs. 19-22. These illustrate that RADAS devices dissipate most of energy on lower stories as shown in Fig. 19, and that VE dampers can dissipate the residual energy further, as shown in Fig. 20. On the other hand, although earthquake induced forces on upper stories are not large enough to yield RADAS devices as shown in Fig. 21, and earthquake induced energy on upper stories still can be reduced by VE dampers as shown in Fig. 22.

7. Conclusions

The main purpose of adding combined energy-absorbing devices to a structure is to mitigate the structural responses in not only earthquake but also in response to wind loadings. Because the characteristics of all kinds of dampers are different, they have particular shortcomings and merits. VE dampers have good performance in wind control and dissipate energy effectively under arbitrary loadings. But VE dampers function less effectively to absorb energy at the early stage of earthquake (due to small or zero velocities). Once the peak of structural seismic responses occurs during the first few seconds of an earthquake, the structural members may be damaged in buildings with only VE dampers. The RADAS device is an optimum selection in large earthquakes. However, when the earthquake is not large enough to cause RADAS devices to yield, RADAS devices will not play an important role in mitigating structural responses. Due to the individual merits of VE dampers and RADAS devices, this paper proposes ways to equip both at the same location. Parametric results reveal that if VE dampers and RADAS devices are combined, their individual shortcomings will be overcome. These devices will function more completely, and the responses of the structure will be reduced more effectively from disturbances ranging from wind and minor earthquakes to severe earthquakes. The combined devices provide a strong fail-safe mechanism.

References

Aiken, I.D., Kelly, J.M. and Pall, A.S. (1988), “Seismic response of a nine-story steel frame with friction

damped cross-bracing", *Report No. UCB/EERC-88/17*, Earthq. Engng. Res. Ctr., Univ. of California at Berkeley, California.
Aiken, I.D., Kelly, J.M. and Mahmoodi, P. (1990), "The application of viscoelastic dampers to seismically resistant structures", *Proc., 4th U.S. Nat. Conf. on Earthq. Engng.,* Palm Springs, California, May, **3**, 459-468.
Bergman, D.M. and Hanson, R.D. (1990), "Viscoelastic versus steel plate mechanical damping devices: An experimental comparison", *Proc. 4th U. S. Nat. Conf. on Earthq. Engng.*, Palm Springs, California, May, **3**, 469-477.
Constantinou, M.C. and Symans, M.D. (1992), "Experimental and analytical investigation of seismic of structures with supplemental fluid viscous dampers", *Report No. NCEER-92-0032*, National Center for Earthquake Engineering Research, SUNY at Buffalo, New York.
FEMA-273 (1997), Federal Emergency Management Agency, NEHRP Guidelines for the Seismic Rehabilitation of Buildings. Federal Emergency Management Agency, Report No. 273 and 274, Washington, D.C., 1997.
Kelly, J.M. and Skinner, M.S. (1980), "The design of steel energy-absorbing restrainers and their incorporation into nuclear power plants for enhanced safety(Vol. 2): Development and testing of restraints for nuclear piping system", *Report No.UCB/EERC-80/21*, Earthq. Engng. Res. Ctr., Univ. of California at Berkeley, California.
Mahmoodi, P. (1972), "Structural dampers", *J. Struct. Div.*, ASCE, **95**(8), 1661-1672.
Pall, A.S., Ghorayeb, F. and Pall, R. (1991), "Friction dampers for rehabilitation of ecole polyvalente at Sorel, Quebec", *Proc., 6th Canadian Conf. On Earthq. Engng*. Toronto, Canada, June, 389-396.
Pekau, O.A. and Guimond, R. (1991), "Controlling seismic response of eccentric structures by friction dampers", *Earthq. Engng. Struct. Dyn.*, **20**(6), 505-521.
Pong, W.S., Tsai, C.S. and Lee, G.C. (1994), "Seismic study of building frames with added energy-absorbing devices", Report No. *NCEER-94-0016*, National Center for Earthquake Engineering Research, State University of New York at Buffalo, New York.
Pong, W.S. and Tsai, C.S. (1995), "Seismic study of buildings with viscoelastic dampers", *An Int. J. Struct. Eng. Mech.*, **3**(6), 569-581.
Skinner, R.I., Kelly, J.M. and Heine, A.J. (1975), "Hysteretic dampers for earthquake-resistant structures", *Earthq. Engng. Struct. Dyn.*, **3**, 287-296.
Soong, T.T. (1998), "Structural control: Impact on structural research in general", *Proc., 2nd World Conf. on Struct. Con.*, Kyoto, Japan, June, **1**, 5-14.
Stiemer, S.F. and Chow, F.L. (1984), "Curved plate energy absorbers for earthquake resistant structures", *Proc., 8th World Conf. on Earthq. Engng*, San Francisco, California, July, **5**, 967-974.
Tsai, C.S. (1993), "Innovative design of viscoelastic dampers for seismic mitigation", *Nuclear Engineering and Design*, **139**, 83-106.
Tsai, C.S. and Lee, H.H. (1993), "Applications of viscoelastic dampers to high-rise buildings", *J. Struct. Engng*, ASCE, **119**(4), 1222-1233.
Tsai, C.S. (1994), "Temperature effect of viscoelastic dampers during earthquakes", *J. Struct. Eng.*, ASCE, **120**(2), 394-409.
Tsai, C.S. and Lee, H.H. (1994), "Applications of viscoelastic dampers to high-rise buildings for seismic mitigation", *J. Struct. Engng.*, ASCE, **120**(12), 3680-3687.
Tsai, C.S. and Tsai, K.C. (1995), "TPEA device as seismic dampers for high-rise buildings", *J. Engng. Mech.*, ASCE, **121**(10), 1075-1081.
Tsai, C.S. and Chung, L.L. (1998), "RADAS as a damper for seismic mitigation", *Proc. of Conf. on Second World Conference on Structural Control*, June, Kyoto, Japan, **1**, 113-120.
Tsai, C.S., Chen, K.C. and Chen, C.S. (1998), "Seismic resistibility of high-rise buildings with combined velocity-dependent and velocity-independent devices", *Proc. of PVP Conference*, ASME, San Diego, California, **366**, 103-110 .
Whittaker, A.S., Bertero, V.V., Alonso, L.J. and Thompson, C. (1989), "Earthquake simulator testing of steel plate added damping and stiffness elements", *Report No. UCB/EERC-89/02*, Earthq. Engng. Res. Ctr., Univ. of California at Berkeley, California.
Zhang, R.H. and Soong, T.T. (1992), "Seismic design of dampers for structural applications", *J. Struct. Engng.*, ASCE, **118**(5), 1375-1392.